

See discussions, stats, and author profiles for this publication at: <https://www.researchgate.net/publication/231650980>

Overstabilization of the Metastable Structure of Isolated Ag–Pd Bimetallic Clusters

ARTICLE *in* THE JOURNAL OF PHYSICAL CHEMISTRY C · OCTOBER 2008

Impact Factor: 4.77 · DOI: 10.1021/jp806604b

CITATIONS

20

READS

30

4 AUTHORS, INCLUDING:



Hyunyou Kim

Chungnam National University

37 PUBLICATIONS 767 CITATIONS

SEE PROFILE



Hyoung Gyu Kim

Korea Advanced Institute of Science and T...

11 PUBLICATIONS 385 CITATIONS

SEE PROFILE

Overstabilization of the Metastable Structure of Isolated Ag–Pd Bimetallic Clusters

Hyun You Kim, Hyoung Gyu Kim, Da Hye Kim, and Hyuck Mo Lee*

Department of Materials Science and Engineering, KAIST, 335 Gwahangno, Yuseong-gu, Daejeon 305-701 Korea

Received: July 25, 2008; Revised Manuscript Received: August 29, 2008

This report on the overstabilization of the metastable structure of isolated Ag–Pd catalyst composed of 135 Ag and 16 Pd atoms is based on a combination of several computational methods such as molecular dynamics, a density functional theory, transition-state calculation, and a modified basin hopping Monte Carlo simulation. With Pd atoms pinned at the metastable position up to the melting point, the overstabilization essentially originated from the systematic interaction of several factors, the high kinetic energy barrier of Pd movement, the low melting temperature of the 135Ag–16Pd cluster, the specific surface morphology, and the low solute concentration. Our results suggest that not only thermodynamics but additional kinetic or structural factors should be considered systematically in deciding the structure of bimetallic clusters for the given conditions.

Introduction

Nanosized bimetallic clusters have superior chemical and physical properties in comparison to nanosized single element clusters.^{1,2} Thus, investigation of the overall morphology and structural stability of bimetallic clusters has attracted much interest in terms of the practical application of bimetallic clusters.^{2–5}

Several computational methods, such as a genetic algorithm, the Monte Carlo method, or a modified basin hopping Monte Carlo (mBHMC) method,⁶ have been used to address the globally stable structure of bimetallic clusters.^{2,3,5–7} The core–shell structure has been confirmed as one of most favorable structures in several bimetallic systems. Reports also confirm that a significant difference in the atomic size and surface energy causes preferential surface segregation of large components with a low surface energy, giving rise to a specific cluster morphology.⁸

In a recent report, Baletto et al. showed that a specific structure of a bimetallic cluster with subsurface-segregated solute atoms can be found in Ag-based bimetallic cluster systems (onionlike structures).⁷ They assumed that this state is metastable because all the solute atoms penetrated into the center of the cluster at a higher temperature. Mariscal et al. also showed the metastability of the onionlike cluster structure.⁹ On the other hand, in our previous study of the coalescence between 135Ag and 16Pd clusters at 500 K, we observed that Pd atoms penetrate the large Ag cluster and that local 5-fold icosahedron (Ih) structures form at the surface.¹⁰ The Pd atoms that penetrated the Ag cluster preferentially segregated at the subsurface layer, mostly beneath the Ih structure, forming an Ih–Pd package composed of one Pd atom and six surrounding Ag atoms. We found that the Ih–Pd package induces a high energy barrier that blocks further movement of the Pd atoms; as a result, the Pd atoms are pinned at the metastable positions. The fact that such a metastable cluster structure was observable at a high temperature (500 K)¹⁰ and showed temperature-dependent stability^{7,9} indicates that another essential factor, kinetics, is also worthy of consideration when dealing with the structure of bimetallic clusters.

There are many experimental and theoretical reports on the catalytic activity of Ag–Pd bimetallic clusters.^{11–18} They are used as selective dehydrogenation catalysts^{13,14} and widely accepted as a replacement of pure Pd catalyst for acetylene hydrogenation in the excess of ethylene in feedstock for ethylene polymerization.¹⁹ Lan et. al showed that the Ag–Pd catalyst has a potential as a new activator for electroless copper deposition.¹⁵ Masuda and co-workers found that the relatively small amount of Pd significantly improves the catalytic activity of Ag clusters for NO_x removal from diesel exhaust gas over a wide range of temperatures using (CH₃)₂O as a reducing agent.¹⁶ Additionally, the Ag–Pd catalyst reduces the nitrogroup of 4-nitrobenzonitrile and 4-nitro-3-pyrazole carboxylic acid to azogroup and aminogroup, respectively.¹⁷ These experimental studies improved our understandings on the Ag–Pd bimetallic catalysts. Surface compositions of catalysts reportedly influence on the binding nature of adsorbates.^{12,13,18} The qualitative role of solute element and structure on the catalytic properties, however, are still in debate.

The chemical properties of bimetallic clusters are reportedly dependent on the overall morphology and solute distribution of the clusters.^{2,11,20} Moreover, because bimetallic clusters can be synthesized by various physical and chemical methods and the final structures can be highly correlated with synthetic sequences,^{2,11,21,22} we focused on the structural stability and solute distribution of bimetallic clusters, which account for the chemical properties.

In this study, we use a combined computational method to examine the structural evolution of Ag–Pd bimetallic clusters in relation to temperature. In particular, we use molecular dynamics (MD) and density functional theory (DFT) with a transition state calculation to interpret the temperature-related dynamic behaviors. The global minimum structure of an Ag–Pd cluster was analyzed with the mBHMC method.⁶

Computational Methods

The MD simulation was carried out at 300, 400, 500, and 700 K under a canonical ensemble with a quantum Sutton–Chen potential,²³ which includes quantum corrections and takes into account the zero-point energy (quantum) effects, thus allowing better prediction of temperature dependent properties.^{24,25} The relevant potential parameters of Ag and Pd together with the

* To whom correspondence should be addressed. E-mail: hmlee@kaist.ac.kr. Phone: +82-42-350-3334. Fax: +82-42-350-3310.

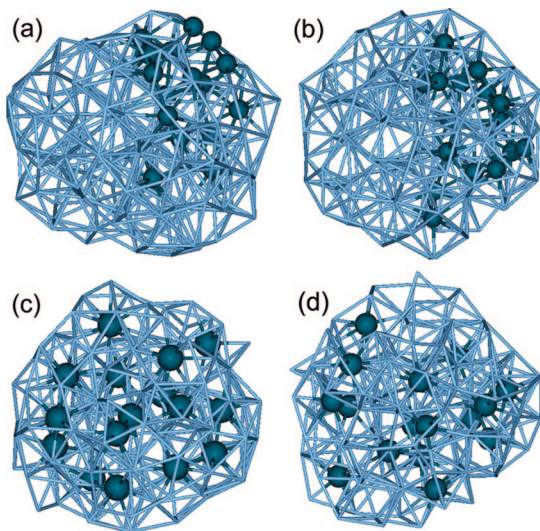


Figure 1. Temperature-dependent internal Pd distribution of the 135Ag–16Pd bimetallic cluster. The structures of clusters were generated after 1 ns of MD simulation at each temperature: (a) 300; (b) 400; (c) 500; (d) 700 K. Light blue lines and dark green spheres represent Ag and Pd atoms, respectively (the same coloring is used throughout the figures).

detailed MD simulation conditions are described in a previous study.⁴ An Ag cluster composed of 135 atoms and a Pd cluster of 16 atoms (at % Pd = 10.6) were individually prepared and fully relaxed at each temperature. The cluster was subsequently placed in a large simulation box (50 nm × 50 nm × 50 nm) where the atoms collided with each other. The diameter of the merged Ag–Pd cluster is around 1.5 nm. The MD simulation of each collision lasted 1000 ps (five million time steps). The mBHC simulation was performed for 20000 MC steps. In more than 100 mBHC tries, the potential global minimum structure was chosen, and it was compared with the MD results. The DFT calculations were performed with the DMol³ package²⁶ in a Materials Studio. The spin-unrestricted Kohn–Sham equation was expanded in a local atomic orbital with a double-numeric quality basis set with polarization functions. The detailed calculation parameters for the geometry optimization and the transition state calculations are described in our previous study.¹⁰

Results

Figure 1 shows the overall structures of the Ag–Pd bimetallic clusters after 1 ns of MD runs at each temperature. The order of internal distribution of the Pd atoms appears to be dependent on the temperature. The Pd atoms penetrated the Ag cluster even at 300 K as reported earlier.⁴ With an increase in temperature, they are clustered at the subsurface (one layer below the surface) layer at 400 K and are dispersed along the subsurface layer at 500 K (the Pd sliding). A cluster at 700 K is similar to the structure at 500 K. The surprising finding is that the Pd atoms that penetrated the Ag cluster are clustered at the subsurface layer at 400 K even after 1 ns and are dispersed along the subsurface layer at 500 and 700 K.

We found that there are no significant differences in the surface layer morphology between 400 and 500 K. Thus, the Pd clustering observed at 400 K has no correlation with the surface morphology of the cluster. The 61 Ag atoms among the 97 and 98 surface atoms were involved in the Ih at 400 and 500 K, respectively. We postulated the existence of very low energy barriers for the Pd penetration and the surface rearrangement in the early stage of

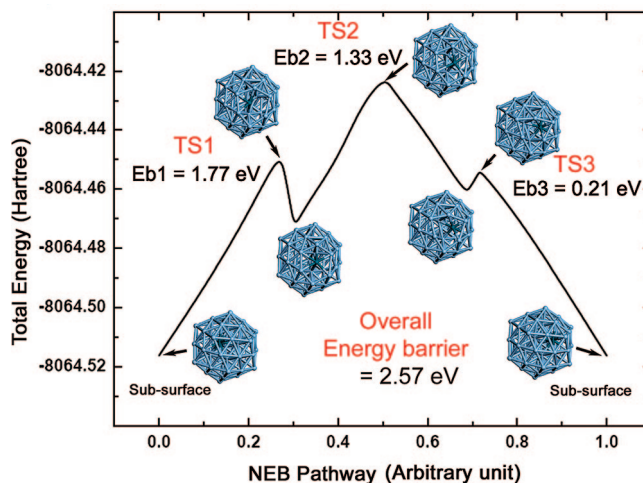


Figure 2. Schematic nudged elastic band pathway and the location of transition states of the internal movement of Pd atom. Each snapshot shows the structural evolution of 55Ih cluster with respect to the Pd movement.

coalescence.⁴ The low-temperature Ih formation at 400 K confirms our finding. On the other hand, parts b and c of Figure 1 indirectly show that there are additional energy barriers for internal Pd movement. These energy barriers could govern the nature of the Pd distribution with temperature.

To rationalize the presence and scale of the energy barriers, we modeled the Ag–Pd cluster with a 55Ih cluster composed of 54 Ag atoms and one Pd atom. The energy of the Ag–Pd–55Ih cluster was found to decrease monotonically as a Pd atom moves from the vertex to the subsurface layer and then to the center of the cluster.¹⁰ Additionally, it was revealed that if an Ih–Pd exists in the surface layer the overall energy barrier against further penetration of an embedded Pd atom is extremely high. Accordingly, the pinning of Pd atoms beneath the surface Ihs observed at 500 K is kinetically reasonable. The overall energy barrier (Eb) of the Pd sliding is as high as 2.57 eV (Figure 2). Although this value is lower than the energy barrier of the Pd penetration, 4.65 eV,¹⁰ the energy barrier of 2.57 eV is too high to be overcome by the rising temperature. Otherwise, the Pd sliding was observed at both 500 and 700 K.

A likely explanation for this phenomenon is the stepped nature of the minimum energy path (MEP). Figure 2 shows three distinguishable transition states (TS1, TS2, and TS3) and two local minimum points on the MEP of the Pd sliding. If we divide the MEP into three independent processes, the energy barriers of each process lie in a considerable range (Eb1 = 1.77 eV, Eb2 = 1.33 eV, and Eb3 = 0.21 eV); this range is comparable with the generally reported energy barriers in catalysis that occurs at around 500 K.²⁷ In general terms, it is appropriate to say that the internal structure of Ag–Pd bimetallic cluster can be associated with the presence of an energy barrier for the movement of Pd atoms.

The melting temperature of a nanosized metal cluster is obviously lower than that of a bulk state.²⁸ Figure 3 confirms that the melting point of the 135Ag–16Pd cluster is around 732 K, which was obtained by the simulated annealing method. Remarkably, the Pd atoms that preferentially segregated at the subsurface layer did not penetrate the center of the cluster at 700 K nor even at a temperature just below the melting point (see Figure 1d and the inset of Figure 3). A core–shell structure was proposed as a substantially stable structure in Ag–Pd clusters;² however, from Figures 1 and 3, we deduce that for a specific condition the metastable cluster structure appears in a

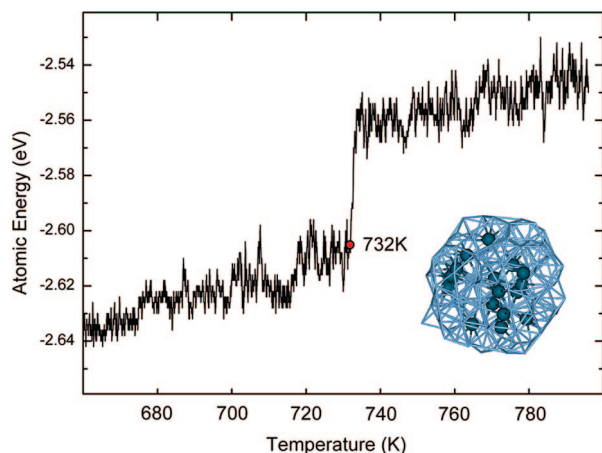


Figure 3. The energy-to-temperature diagram showing a solid to liquid transition of the 135Ag–16Pd bimetallic cluster. The Ag–Pd cluster underwent simulated annealing from 300 to 800 K with 20 K of temperature steps with 100 ps of stabilization time at each temperature. The melting point is 732 K, and the inset shows the cluster structure at 720 K.

wide temperature range, up to just below the melting point. We found that the very high energy barrier along the cluster axis consequently restricts the internal movement of the Pd atoms along the axis of the cluster. The metastable structure can therefore be overstabilized up to the melting point. Because only the Pd sliding is kinetically allowed, Pd atoms prefer to move along the subsurface layer rather than to penetrate into the center of the cluster even at high temperatures (500 and 700 K) and pinned below surface Ihs.

The potential global minimum structure of the 135Ag–16Pd bimetallic cluster obtained from the mBHC method gives credence to the above findings. Figure 4 shows the most stable geometry of the 135Ag–16Pd bimetallic cluster that is found in more than 100 mBHC tries. The Pd atoms were not segregated at the subsurface layer but substantially penetrated the center of the cluster, where they formed the Pd core. In addition, as the Pd atoms migrate to the center of the cluster, the Ag atoms of the close-packed surface Ihs were disordered and rearranged to triangular (111) surfaces. Because our cluster has only four more atoms than a general 147Ih, the final structure is close to 147Ih. Clearly, there is a close relation between the stability of the surface Ihs and the location of the Pd atoms. In general, the nature of the solute distribution of a bimetallic cluster is governed by the surface morphology and vice versa. Ferrando and co-workers showed the special stability of poly-Ih bimetallic clusters which both maximize the bond number and minimize the strain.²⁹ Very recently, moreover, Yuan et al. reported the peculiar distribution pattern of Pd atoms in the Au–Pd bimetallic cluster system.³⁰ We also found that at 500 K the surface layer of Ag–Au and Ag–Pt clusters is covered with Ihs and that the solute atoms are segregated at the subsurface layer.³¹ These correlations consequently account for the chemical properties of bimetallic clusters, such as the catalytic activity, because the properties of the clusters are a kind of manifestation of their structure.^{2,20}

Discussion

Even the most extensive studies on bimetallic clusters have until now dealt mainly with the global minimum structure. There are very few reports on the metastable structure.^{7,9,32,33} If we consider the fact that the overall cluster morphology of a bimetallic cluster can be varied with the synthetic process, we

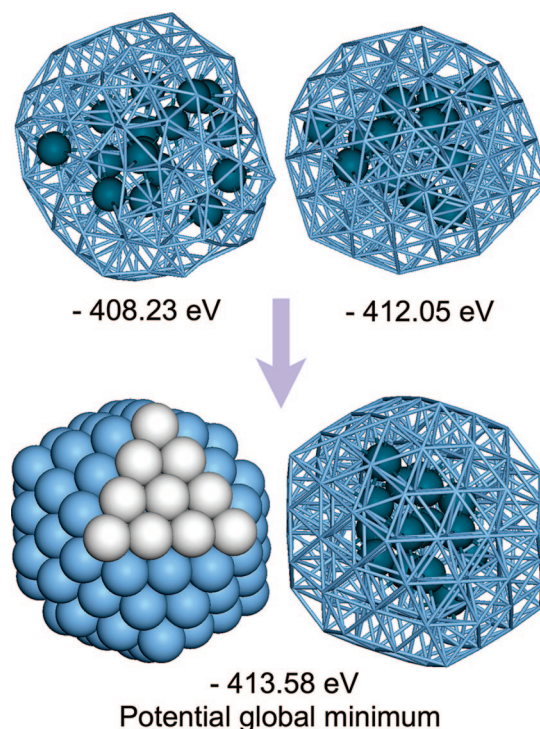


Figure 4. Structural evolution of the 135Ag–16Pd bimetallic cluster. The potential global minimum with core–shell structure was attained. The Pd atoms apparently formed the cluster core. Surface Ag atoms were rearranged into the triangular (111) surfaces as the Pd atoms migrate into the cluster center.

can expect the synthesis of metastable clusters to be dependent on the method, resulting in an abnormal level of overstabilization. Some experimental findings on the surface morphology of the Ag–Pd catalyst cluster are in parallel with our postulations. Khan et al. synthesized an alumina-supported Ag–Pd bimetallic cluster by using the physical vapor deposition method; they reportedly found an alloy Ag–Pd bimetallic cluster rather than a core–shell type at room temperature.¹¹ Note also that Khan et al.¹¹ predicted the presence of an isolated Pd atom surrounded by Ag atoms on the surface of the cluster. These experimental findings, namely, the formation of the alloy cluster at room temperature and the presence of the isolated Pd atom surrounded by Ag atoms, are in agreement with the overall cluster structure of our metastable Ag–Pd cluster. Our cluster shows an alloyed structure rather than a core–shell and has localized Pd atoms surrounded by Ag atoms (Ih–Pd) on the surface.

Isolation of solute atoms is not an exclusive phenomenon of the Ag–Pd system. The isolation of Pd atoms at the surface of the Au–Pd catalyst was reported as well.^{21,30,34} In addition, after consideration of the recent experimental and theoretical reports on the Au–Pd or Ag–Pd systems by Yuan et al.,³⁰ Khan et al.,^{11,18} Neurock and co-workers,¹³ Chen et al.,³⁴ Gonzalez et al.,¹² and Mejia-Rosales et al.,²¹ we conclude that the isolated atoms alter the local electronic state of the catalyst surface and thus that they are responsible for the improved and localized catalytic activity of bimetallic clusters. The overstabilized 135Ag–16Pd cluster, which we are reporting here, also has the localized Pd atoms at the subsurface layer. We expect therefore that the overstabilized Ag–Pd cluster has distinguishable catalytic properties compared to the pure Ag cluster or the Ag–Pd core–shell cluster.

In a previous report, we suggested an efficient way of finding the solid-to-liquid transition region.²⁸ By use of this method,

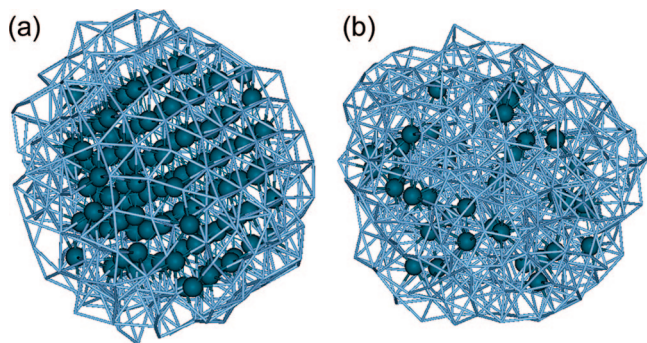


Figure 5. Morphology of the Ag–Pd bimetallic clusters (diameter \approx 2.2 nm) at 60 K below their melting temperatures: (a) 30 at % Pd at 780 K and (b) 10 at % Pd at 710 K.

we can monitor the sequential solid state transition of a bimetallic cluster until it melts. We found that a 2.2-nm-sized Ag–Pd bimetallic cluster with a Pd concentration of 30 at % has a perfect core–shell structure (see Figure 5a). Interestingly, however, when the Pd concentration is low (10 at %), the Pd atoms tend to be dispersed at the subsurface layers rather than cohere and form a Pd core, even before the cluster melts (see Figure 5b). Parts a and b of Figure 5 represent the cluster structures at 780 and 710 K, respectively, which is about 60 K below the melting point of each cluster. It is not clear yet whether the solute concentration is another factor that controls the internal structure of the cluster morphology. However, we hypothesized that the solute concentration should be taken into account when dealing with the structure of a bimetallic cluster at a given condition. We assume that the movement of Pd atoms is mainly governed by the energy barrier, that is the kinetic factor, and not by the interaction between atoms when the Pd concentration is low.

The low melting temperature of the 135Ag–16Pd system could be a likely explanation for overstabilization of the metastable structure. In the initial 10000 steps of our mBHC simulations, each atom was allowed to have a high thermal energy that is equal to 3000 K not to be trapped at a local minimum. In fact, the melting temperature of 135Ag–16Pd is quite low, 732 K (see Figure 3). We speculate that, because its melting temperature is low, the cluster would melt before the Pd atoms have a sufficient thermal energy and thus the cluster reach the global minimum.

On the basis of the combined computational results, we propose the following:

(1) The high energy barrier for the solute movement, which cannot be overcome by the rising temperature, is an essential factor in the overstabilization of the metastable cluster structure at high temperature.

(2) The origin of the high energy barrier is related to the specific surface morphology, such as the surface Ihs.

(3) The stability of the surface Ihs is correlated with the presence of the Pd atoms that segregate at the subsurface layer.

(4) The low melting temperature of the 135Ag–16Pd cluster contributes to the overstabilization of the metastable structure up to the melting point.

(5) The low solute concentration contributes to the abnormal stability of the metastable structure.

In summary, we found that the metastable structure of an Ag–Pd bimetallic cluster can be overstabilized up to the melting point because of kinetic reasons. Our findings indicate that under specific conditions the internal structure of bimetallic clusters may differ from the structure that occurs at their thermodynamic

ally most stable state. To the best of our knowledge, there have been very few substantial studies on the metastable structure of bimetallic clusters. In addition, there are numerous environmental factors, such as the temperature, the concentration of the cluster, the pressure of the catalytic reactant, and the adsorbate-induced surface segregation,³⁵ that could influence the cluster structure. We deduce therefore that consideration should not be limited solely to the globally minimized cluster structure when dealing with bimetallic clusters for practical applications. Rather, for the synthesis and application of bimetallic clusters, we suggest that consideration should be extended systematically to kinetic and structural factors. The overstabilization of the metastable structure of the Ag–Pd cluster is a typical example. Questions still remain with regard to the most dominant factor that controls the overstabilization of the metastable cluster structure and whether the observed behavior is a general phenomenon in every bimetallic cluster system.

Acknowledgment. This work was supported by the Korea Science and Engineering Foundation (KOSEF) grant funded by the Korea government (MEST) (No. R01-2008-000-10986-0).

References and Notes

- (1) (a) Alivisatos, A. P. *J. Phys. Chem.* **1996**, *100*, 13226. (b) Mavrikakis, M.; Hammer, B.; Norskov, J. K. *Phys. Rev. Lett.* **1998**, *81*, 2819. (c) Mizukoshi, Y.; Fujimoto, T.; Nagata, Y.; Oshima, R.; Maeda, Y. *J. Phys. Chem. B* **2000**, *104*, 6028. (d) Sinfelt, J. H. *Bimetallic Catalysts: Discoveries, Concepts, and Applications*; Wiley: New York, 1983.
- (2) Ferrando, R.; Jellinek, J.; Johnston, R. L. *Chem. Rev.* **2008**, *108*, 845.
- (3) Cheng, D. J.; Wang, W. C.; Huang, S. P. *J. Phys. Chem. B* **2006**, *110*, 16193.
- (4) Kim, H. Y.; Lee, S. H.; Kim, H. G.; Ryu, J. H.; Lee, H. M. *Mater. Trans.* **2007**, *48*, 455.
- (5) Lloyd, L. D.; Johnston, R. L.; Salhi, S.; Wilson, N. T. *J. Mater. Chem.* **2004**, *14*, 1691.
- (6) Kim, H. G.; Choi, S. K.; Lee, H. M. *J. Chem. Phys.* **2008**, *128*, 144702.
- (7) Baletto, F.; Mottet, C.; Ferrando, R. *Phys. Rev. Lett.* **2003**, *90*, 135504.
- (8) (a) Baletto, F.; Mottet, C.; Ferrando, R. *Phys. Rev. B* **2002**, *66*, 155420. (b) Ruban, A. V.; Skriver, H. L.; Norskov, J. K. *Phys. Rev. B* **1999**, *59*, 15990. (c) Lovvik, O. M. *Surf. Sci.* **2005**, *583*, 100. (d) Rapallo, A.; Rossi, G.; Ferrando, R.; Fortunelli, A.; Curley, B. C.; Lloyd, L. D.; Tarbuck, G. M.; Johnston, R. L. *J. Chem. Phys.* **2005**, *122*, 194308. (e) Rossi, G.; Ferrando, R.; Rapallo, A.; Fortunelli, A.; Curley, B. C.; Lloyd, L. D.; Johnston, R. L. *J. Chem. Phys.* **2005**, *122*, 194309.
- (9) Mariscal, M. M.; Dassie, S. A.; Leiva, E. P. M. *J. Chem. Phys.* **2005**, *123*, 184505.
- (10) Kim, H. Y.; Kim, H. G.; Ryu, J. H.; Lee, H. M. *Phys. Rev. B* **2007**, *75*, 212105.
- (11) Khan, N. A.; Uhl, A.; Shaikhutdinov, S.; Freund, H.-J. *Surf. Sci.* **2006**, *600*, 1849.
- (12) Gonzalez, S.; Neyman, K. M.; Shaikhutdinov, S.; Freund, H.-J.; Illas, F. *J. Phys. Chem. C* **2007**, *111*, 6852.
- (13) Sheth, P. A.; Neurock, M.; Smith, C. M. *J. Phys. Chem. B* **2005**, *109*, 12449.
- (14) Zea, H.; Lester, K.; Datye, A. K.; Rightor, E.; Gulotty, R.; Waterman, W.; Smith, M. *Appl. Catal., A* **2005**, *282*, 237.
- (15) Lan, J.-L.; Wan, C.-C.; Wang, Y.-Y. *J. Electrochem. Soc.* **2008**, *155*, K77.
- (16) Masuda, K.; Shinoda, K.; Kato, T.; Tsujimura, K. *Appl. Catal., B* **1998**, *15*, 29.
- (17) Pergolese, B.; Muniz-Miranda, M.; Bigotto, A. *Chem. Phys. Lett.* **2007**, *438*, 290.
- (18) Khan, N. A.; Shaikhutdinov, S. K.; Freund, H.-J. *Catal. Lett.* **2006**, *108*, 159.
- (19) (a) Frevel, L. K.; Kressley, L. J. Selective Hydrogenation of Acetylene in Ethylene and Catalyst Therefore. US Patent, 1957. (b) Johnson, M. M.; Walker, D. W.; Nowack, G. P. Selective Hydrogenation Catalyst. US Patent, 1983.
- (20) (a) Khanra, B. C.; Bertolini, J. C.; Rousset, J. L. *J. Mol. Catal. A* **1998**, *129*, 233. (b) Kitchin, J. R.; Khan, N. A.; Barteau, M. A.; Chen, J. G.; Yakshinskiy, B.; Madey, T. E. *Surf. Sci.* **2003**, *544*, 295.

- (21) Mejia-Rosales, S. J.; Fernandez-Navarro, C.; Perez-Tijerina, E.; Blom, D. A.; Allard, L. F.; Jose-Yacaman, M. *J. Phys. Chem. C* **2007**, *111*, 1256.
- (22) Ferrer, D.; Torres-Castro, A.; Gao, X.; Sepulveda-Guzman, S.; Ortiz-Mendez, U.; Jose-Yacaman, M. *Nano Lett.* **2007**, *7*, 1701.
- (23) Qi, Y.; Cagin, T.; Kimura, Y.; Goddard, W. A. *J. Comput.-Aided Mater. Des.* **2002**, *8*, 233.
- (24) Cagin, T.; Kimura, Y.; Qi, Y.; Li, H.; Ikeda, H.; Johnson, W. L.; Goddard W. A.; *Bulk Metallic Glasses, MRS Symposia Proceedings No.554*; Johnson, W. L., Liu, C. T., Inoue, A. Materials Research Society: Pittsburgh, 1999.
- (25) Qi, Y.; Cagin, T.; Kimura, Y.; Goddard, W. A., III. *Phys. Rev. B* **1999**, *59*, 3527–3533.
- (26) (a) Delley, B. *J. Phys. Chem.* **1996**, *100*, 6107. (b) Delley, B. *J. Chem. Phys.* **2000**, *113*, 7756.
- (27) (a) Feng, T.; Vohs, J. M. *J. Catal.* **2002**, *208*, 301. (b) Dobler, J.; Pritzsche, M.; Sauer, J. *J. Am. Chem. Soc.* **2005**, *127*, 10861.
- (28) Kim, D. H.; Kim, H. Y.; Kim, H. G.; Ryu, J. H.; Lee, H. M. *J. Phys.: Condens. Matter* **2008**, *20*, 035208.
- (29) Rossi, G.; Rapallo, A.; Mottet, C.; Fortunelli, A.; Baletto, F.; Ferrando, R. *Phys. Rev. Lett.* **2004**, *93*, 105503.
- (30) Yuan, D. W.; Gong, X. G.; Wu, R. Q. *Phys. Rev. B* **2008**, *78*, 035441.
- (31) Ryu, J. H.; Kim, H. Y.; Kim, D. H.; Choi, S. K.; Lee, H. M. *J. Nanosci. Nanotechnol.* Accepted.
- (32) Wang, J. L.; Ding, F.; Shen, W. F.; Li, T. X.; Wang, G. H.; Zhao, J. *J. Solid State Commun.* **2001**, *119*, 13.
- (33) Yang, L. Q. *Phil. Mag. A* **2000**, *80*, 1879.
- (34) Chen, M. S.; Kumar, D.; Yi, C. W.; Goodman, D. W. *Science* **2005**, *310*, 291.
- (35) Soto-Verdugo, V.; Metiu, H. *Surf. Sci.* **2007**, *601*, 5332.

JP806604B